

RESEARCH

Open Access



Esketamine attenuates traumatic brain injury by modulating STAT3-mediated Glycolysis and immune responses

Yufang Liu^{1†}, Zheng Gong^{2†}, Longfei Zhang¹, Xian Yang³, Jie Zhu¹, Xin Zhou¹ and Xingzhi Liao^{1*}

Abstract

Background Secondary injury following traumatic brain injury (TBI) involves neuroinflammation, immune cell infiltration, and metabolic dysregulation, leading to progressive neurological damage. This study evaluates the potential of esketamine, an NMDA receptor antagonist, to modulate immune responses, inhibit glycolysis, and mitigate secondary brain injury in a TBI mouse model.

Methods Male C57BL/6J mice were subjected to controlled cortical impact to induce TBI. Mice were treated with esketamine, either alone or combined with the STAT3 activator colivelin, or the glycolysis inhibitor 2-deoxyglucose (2-DG). Neurological function, BBB permeability, immune cell infiltration, macrophage polarization, and glycolytic activity were assessed using immunohistochemistry, flow cytometry, quantitative PCR, and enzyme-linked immunosorbent assay (ELISA).

Results Esketamine treatment significantly reduced structural brain tissue damage, including contusions, tissue loss, and edema, while also improving neurological outcomes in TBI mice. Mechanistically, esketamine inhibited CD4+T cell activation and suppressed Th17 differentiation both in vivo and in vitro. It also promoted a shift in macrophage polarization from the pro-inflammatory M1 phenotype to the anti-inflammatory M2 phenotype. Further analysis revealed that esketamine blocked STAT3 activation, which in turn reduced the expression of glycolytic genes (e.g., Hk2, Pfkfb3, Aldoa) essential for Th17 cell proliferation and M1 polarization. Co-treatment with colivelin reversed esketamine's effects on STAT3-mediated glycolysis, while 2-DG enhanced its anti-inflammatory actions.

Conclusion Esketamine attenuates TBI-induced neuroinflammation and tissue damage by inhibiting STAT3-mediated glycolysis, thus reducing Th17 and M1 macrophage activity and promoting regulatory and reparative immune responses. These findings highlight esketamine's potential as a therapeutic option for TBI, targeting both immune modulation and metabolic pathways to alleviate secondary injury.

Clinical trial number not applicable.

Keywords Traumatic brain injury, Esketamine, STAT3, Immune modulation, Glycolysis

[†]Yufang Liu and Zheng Gong contributed equally to this work.

*Correspondence:
Xingzhi Liao
liaoxingzhi@aliyun.com

¹Department of Anesthesiology, 904th Hospital of The Joint Logistics Support Force of the PLA, No. 101, North Xingyuan Rd, Liangxi District, Wuxi, Jiangsu 214044, P. R. China

²Department of Anesthesiology, Changzhou Medical Area, 904th Hospital of The Joint Logistics Support Force of the PLA, Wuxi, Jiangsu 214044, P. R. China

³Anhui Medical University, Hefei, Anhui 230032, P. R. China



Background

Traumatic brain injury (TBI) results from the external pressure or force that traumatically injures the brain [1]. TBI is a major health and socioeconomic concern as it is one of the world's leading causes of mortality and disability, particularly among youth [2]. TBI consists of two types of injuries: the primary injuries, such as blood-brain barrier (BBB) disruption and cerebral edema development, and the secondary injuries, which result in the loss of neuronal cells and are caused by a complex series of interacting cascades, including inflammation, stress, and apoptosis. More importantly, TBI can induce significant motor, sensory, cognitive and emotional impairments [3]. A substantial benefit is not seen after drug interventions, despite the fact that a growing number of randomized controlled trials, including those involving intracranial pressure monitoring, therapeutic hypothermia, surgical techniques, and drug administration, have been conducted recently and the long-term outcome has significantly improved [1, 4–6]. That is why it is crucial and required to conduct research aimed at elucidating the pathophysiological mechanisms of TBI and identifying novel targets for pharmacological interventions.

Following central nervous system (CNS) injury, T cells can develop into pro-inflammatory T cell subsets (such as T helper T cell 1 (Th1) or Th17) or anti-inflammatory T cell subsets (i.e. Th2 or T regulatory T cells (Treg)) through cytokine production by macrophages [7]. Variations in T cell subsets have been linked to the pathophysiology of TBI and have been demonstrated to impact immunological responses [8]. In addition, research has shown that facilitating the shift of macrophages and microglia from the M1 phenotype to the M2 phenotype can lessen brain injury [9, 10]. Yet, the regulation of the innate immune response and the polarization of macrophage M1/M2 in TBI has not been addressed.

Esketamine, an enantiomer of ketamine, functions as a potent analgesic and antagonist of the N-methyl-D-aspartate (NMDA) receptor, targeting excitatory pathways involved in neurotoxicity and inflammation [11]. While originally recognized for its anesthetic properties, esketamine has recently been approved by the FDA for treatment-resistant depression due to its rapid and unique antidepressant effects, which arise from modulating glutamatergic neurotransmission and enhancing synaptic connectivity [12]. Beyond these clinical uses, a growing body of evidence suggests that esketamine also exerts significant neuroprotective and anti-inflammatory effects, particularly in the context of neuroinflammatory and neurodegenerative conditions. For example, studies indicate that esketamine can enhance hippocampal neurogenesis, improve neuronal survival, and promote neuroplasticity, contributing to cognitive recovery after injury.

Esketamine's neuroprotective mechanism is thought to involve multiple signaling pathways beyond NMDA receptor antagonism. For instance, esketamine has been found to improve cognitive function by activating the STING/TBK1 pathway, a key regulator of cellular stress responses that helps modulate neuroinflammatory processes post-surgery [13]. Additionally, esketamine has been shown to suppress microglia-mediated neuroinflammation by activating the brain-derived neurotrophic factor (BDNF) pathway, which promotes neuronal resilience and cognitive function, particularly in inflammatory models such as sepsis-associated encephalopathy [14]. Given that neuroinflammation and cellular stress responses are also central to the progression of TBI, these findings suggest that esketamine could be a promising candidate for mitigating TBI-induced damage.

Based on these insights, our hypothesis posits that esketamine may alleviate secondary injuries and inflammation in TBI through the modulation of CD4⁺ T cell differentiation and macrophage polarization. This study explores the effects of esketamine on brain tissue defects, inflammation, and immune cell dynamics in a TBI mouse model. We focus on the impact of esketamine on Th17 and Treg responses and macrophage polarization, examining the underlying mechanisms *in vitro*, particularly the role of STAT3-mediated glycolysis in regulating immune cell function.

Methods

Animals and grouping

We used adult male C57BL/6J mice, aged 8–10 weeks and weighing 22–25 g, bought from Vital River Laboratories Animal Technology Co. Ltd (Beijing, China). The animals were housed under controlled conditions, with *ad libitum* access to food and water, a regulated temperature of 25 ± 2 °C, $55 \pm 5\%$ humidity, and a 12-hour light/dark cycle. A total of 30 mice were divided into five groups (6 mice/group): Sham, TBI, TBI + Esk, TBI + Esk + anti-IL-17 A, and TBI + Esk + Colivelin (a selective STAT3 agonist). All the operations followed the National Institutes of Health Guidelines for the Care and Use of Laboratory Animals and ARRIVE Guidelines pertaining to animal experimentation. All animal experiments were approved by the Animal Ethics Committee of 904th Hospital of The Joint Logistics Support Force of the PLA (20241201).

TBI model

Moderate TBI was induced using the controlled cortical impact (CCI) model, as previously described [15]. Briefly, mice were anesthetized with an intraperitoneal injection of 250 μ L of 2.5% tribromoethanol (Sigma, T48402), and a 5-mm craniotomy was performed in the left parietal cortex, centered between bregma and the lambdoid suture. TBI was induced with an aerodynamic impact

device (PSI, USA), using a 3-mm metal tip at 3.5 m/s to the dura. The scalp was closed, and the craniotomy site was covered with medical bone wax. Mice were sacrificed 72 h post-TBI with an intraperitoneal injection of 100 mg/kg sodium pentobarbital. In the Sham group, only a craniotomy was performed without impact.

Drug administration

Esketamine was obtained from Hengrui Pharmaceutical Co. (Jiangsu, China). The first dose of esketamine (4 mg/kg) was administered intraperitoneally 30 min post-TBI, followed by a second dose 24 h later. Daily injections continued for seven days. This dosing schedule was selected based on previous research [16] demonstrating the neuroprotective effects of esketamine when administered within a similar timeframe. Esketamine was dissolved in saline, and saline was also administered to Sham and TBI groups as a vehicle control.

For anti-IL-17 A treatment, mice received 100 µg of anti-IL-17 A via intraperitoneal (i.p.) injection 24 h prior to TBI induction to effectively neutralize IL-17 A-mediated inflammation during the early immune response phase.

For colivelin treatment, mice were administered 1 mg/kg of colivelin daily for 14 consecutive days via intraperitoneal (i.p.) injection following TBI induction. Colivelin was used as a selective STAT3 activator to assess its role in modulating esketamine's effects on STAT3-mediated glycolysis and immune responses.

Evans blue extravasation assay

BBB permeability was assessed by measuring Evans Blue (EB) dye extravasation in brain tissue three days post-TBI. Mice were anesthetized two hours after an intravenous injection of EB dye (2%, 2 µL/g, MedChemExpress, HY-B1102). Following intraventricular perfusion with PBS to clear residual dye, brain tissue was harvested, weighed, and homogenized in formamide (200 mg tissue/mL). After a 48-hour incubation at 37 °C, samples were centrifuged at 5000 rpm for 15 min, and the supernatant absorbance was measured at 632 nm using a spectrophotometer (BioTek, USA).

Haematoxylin and Eosin (H&E) staining

Brain tissue samples were snap-frozen in liquid nitrogen, rinsed with PBS, fixed in 4% formaldehyde, and embedded in paraffin. Paraffin Sect. (4 µm thick) were stained with hematoxylin (1:2) for two minutes, followed by 0.3% acid alcohol treatment and eosin counterstaining. Images were captured using a BX51 microscope (Olympus).

Modified neurological severity score (mNSS)

Neurological function was evaluated 72 h post-TBI using a modified neurological severity score (mNSS) system,

which includes motor, sensory, reflex, and balance tests [1]. Scoring was conducted by a blinded observer, with scores ranging from 0 to 18; higher scores indicated worse neurological function.

CD4+T cell isolation and differentiation in vitro

CD4+T cells were isolated from the spleens of normal and TBI mice using a CD4+T cell isolation kit (STEM-CELL, Canada). Cells were cultured in RPMI-1640 medium with 10% FBS and pre-coated plates with anti-mouse CD3 and CD28 antibodies (Biolegend, USA). For Treg differentiation, 10 ng/mL TGF-β was added, while Th17 differentiation was induced with 50 ng/mL IL-6, 2.5 ng/mL TGF-β, 5 µg/mL anti-IFN-γ, and 5 µg/mL anti-IL-4 (all Biolegend, USA). Prior to culture, cells were labeled with CFSE to monitor proliferation.

Flow cytometric analysis for the proportions of Th17 and Treg cells

Lymphocytes were isolated from spleens, washed with PBS, and stained with FITC-labeled CD4 and APC-labeled CD25 antibodies (BD Biosciences, USA). Cells were then incubated with PMA, ionomycin, and monensin (MultiSciences, China), fixed, permeabilized, and stained with PE-labeled antibodies for IL-17 A, RORγt, and FOXP3 (BD and eBioscience). Data were collected using a FACS Calibur flow cytometer (Beckman Coulter, USA) and analyzed with FlowJo software.

Bone-marrow-derived macrophages (BMDMs) isolation and culture

Bone marrow cells were harvested from freshly collected mouse femurs, filtered, and treated with red blood cell lysis buffer [17]. Cells were cultured in RPMI-1640 with 10% FBS and 50 ng/mL M-CSF for seven days to obtain mature BMDMs. RAW264.7 cells, a monocyte-derived macrophage cell line, were obtained from the Cell Bank of the Chinese Academy of Sciences and cultured in similar conditions.

Flow cytometric analysis for macrophage polarization

RAW264.7 and BMDM cells were seeded, activated with LPS for 24 h, and treated with different concentrations of esketamine. Cells were stained with F4/80, CD86, and CD206 antibodies, and analyzed using flow cytometry and FlowJo software.

Cells treatment

CD4+T cells, RAW264.7, and BMDM cells were cultured with Esk (20, 40, 80 µg/mL) or PBS for four days. CD4+T cells were also cultured under Th17-polarizing conditions with or without 0.5 µM colivelin (MedChemExpress, HY-P1061), a STAT3 activator. RAW264.7 cells were treated with LPS (1 µg/mL) in the presence or

absence of 2-deoxyglucose (2-DG, 4 μ M, Sigma-Aldrich, D8375), a glycolysis inhibitor.

Quantitative real-time PCR (qRT-PCR)

Total RNA was extracted using Trizol reagent, and cDNA was synthesized using a cDNA synthesis kit (Takara, Japan). qRT-PCR was conducted with SYBR Premix Ex Taq II (Takara) on a ViiA 7 Dx system (Applied Biosystems). Gene expression was normalized to GAPDH using the $2^{-\Delta\Delta C_t}$ method. Primer sequences are listed in Table S1.

Western blotting

Cells were lysed and proteins were measured via BCA assays. We separated proteins using 10% SDS-PAGE gels and transported onto PVDF membranes. Membranes were probed with anti-STAT3 (ab68153; dilution 1:1000, Abcam), anti-p-STAT3 (phospho Y705; ab267373; dilution 1:1000, Abcam), and anti- β -actin (ab8227, dilution 1:3000) at 4 $^{\circ}$ C for 24 h. Following incubation with HRP-conjugated secondary antibodies (ab6721, dilution 1:2500, Abcam), blots were developed using BeyoECL Moon enhanced chemiluminescence kits (Beyotime). For densitometric analysis, proteins were normalized to the corresponding total protein level. Representative data from three independent experiments yielding comparable results are shown ($n = 3$).

Enzyme-linked immunosorbent assay (ELISA)

Following the manufacturer's instructions, ELISA was used to assess the levels of mouse IL-1 β (cat. no. ab197742; Abcam), IL-6 (cat. no. ab222503; Abcam), and TNF α (cat. no. ab208348; Abcam).

Immunofluorescence staining

For immunofluorescence analysis, tissue sections or cell smears are fixed with 4% Paraformaldehyde and permeabilized with 0.2% Triton X-100, blocked with 2% BSA for 30 min and then incubated with primary antibody at 4 $^{\circ}$ C for the entire night. The following primary antibodies were used: anti-mouse CD206 (1:500, ab183685, Abcam, UK), anti-mouse INOS (1:500, ab178945, Abcam), anti-mouse STAT3 (1:200, ab68153, Abcam), and rabbit F4/80 antibody (1:400; CST, 30325T). Subsequently, sections were incubated with species-specific Alexa Fluor-coupled secondary antibody IgG conjugated to the Alexa Fluor 488 (ab150077, Abcam) for 2 h at room temperature.

Cell viability assay

A CCK-8 assay was used to assess cell viability. Cells were plated at 50,000 cells per well in 96-well plates, treated with LPS and various concentrations of Esk, followed by CCK-8 solution for four hours. Absorbance at 450 nm was measured to determine viability.

Statistical analysis

Data are presented as mean \pm SD. Analyses were performed using GraphPad Prism. Normality was assessed using the Shapiro-Wilk test, and all data met the normality assumption ($p > 0.05$). Consequently, parametric tests were used for statistical comparisons. For comparisons between two groups, Student's t-test was used, while one-way ANOVA with Tukey's post hoc test was used for multiple groups. For cell experiments, each experiment was repeated three times, with at least three mice per group for each experiment. A p -value ≤ 0.05 was considered statistically significant.

Results

Esketamine alleviates brain tissue defects

Following TBI, brain tissue defects typically develop in the injured area, with more extensive tissue damage resulting in greater neural function loss [18]. To assess the integrity of the BBB, which is often disrupted following TBI, Evans Blue (EB) extravasation was used as a measure of BBB permeability [19]. After 21 days of TBI, mice treated with esketamine exhibited significantly reduced EB extravasation in the injured hemispheres compared to the TBI group (TBI + Esk: 0.58 ± 0.15 μ g/g tissue vs. TBI: 1.25 ± 0.21 μ g/g tissue, $p < 0.01$; Fig. 1A, B), indicating a reduction in BBB permeability. To further evaluate the extent of brain tissue damage, we examined H&E-stained coronal sections from mice brains, focusing on slices with the largest observable defects. Esketamine treatment reduced the extent of brain tissue abnormalities in TBI mice (Fig. 1C, D), suggesting a protective effect on brain structure.

Esketamine alleviates inflammation

Additionally, we assessed the expression levels of inflammatory markers in the brain tissue by quantifying the mRNA levels of IL-1 β , TNF- α , and IL-6. Compared to the sham group, TBI significantly increased the expression of these pro-inflammatory cytokines (IL-1 β : 2.85 ± 0.32 , TNF- α : 2.51 ± 0.28 , and IL-6: 3.02 ± 0.35 , all $p < 0.001$). Esketamine treatment significantly lowered the mRNA expression levels of IL-1 β (1.45 ± 0.25 , $p < 0.001$), TNF- α (1.38 ± 0.22 , $p < 0.01$), and IL-6 (1.65 ± 0.27 , $p < 0.001$) compared to the untreated TBI group (Fig. 2A).

To confirm these findings at the protein level, we measured serum concentrations of IL-1 β , TNF- α , and IL-6 using ELISA. Consistent with the mRNA results, TBI mice displayed elevated levels of these cytokines in the serum (IL-1 β : 315 ± 28 pg/ml, TNF- α : 288 ± 32 pg/ml, IL-6: 210 ± 25 pg/ml, all $p < 0.001$ compared to sham). Esketamine treatment significantly reduced serum levels of IL-1 β (156 ± 18 pg/ml, $p < 0.001$), TNF- α (172 ± 21 pg/ml, $p < 0.001$), and IL-6 (142 ± 20 pg/ml, $p < 0.01$) compared to the TBI group (Fig. 2B).

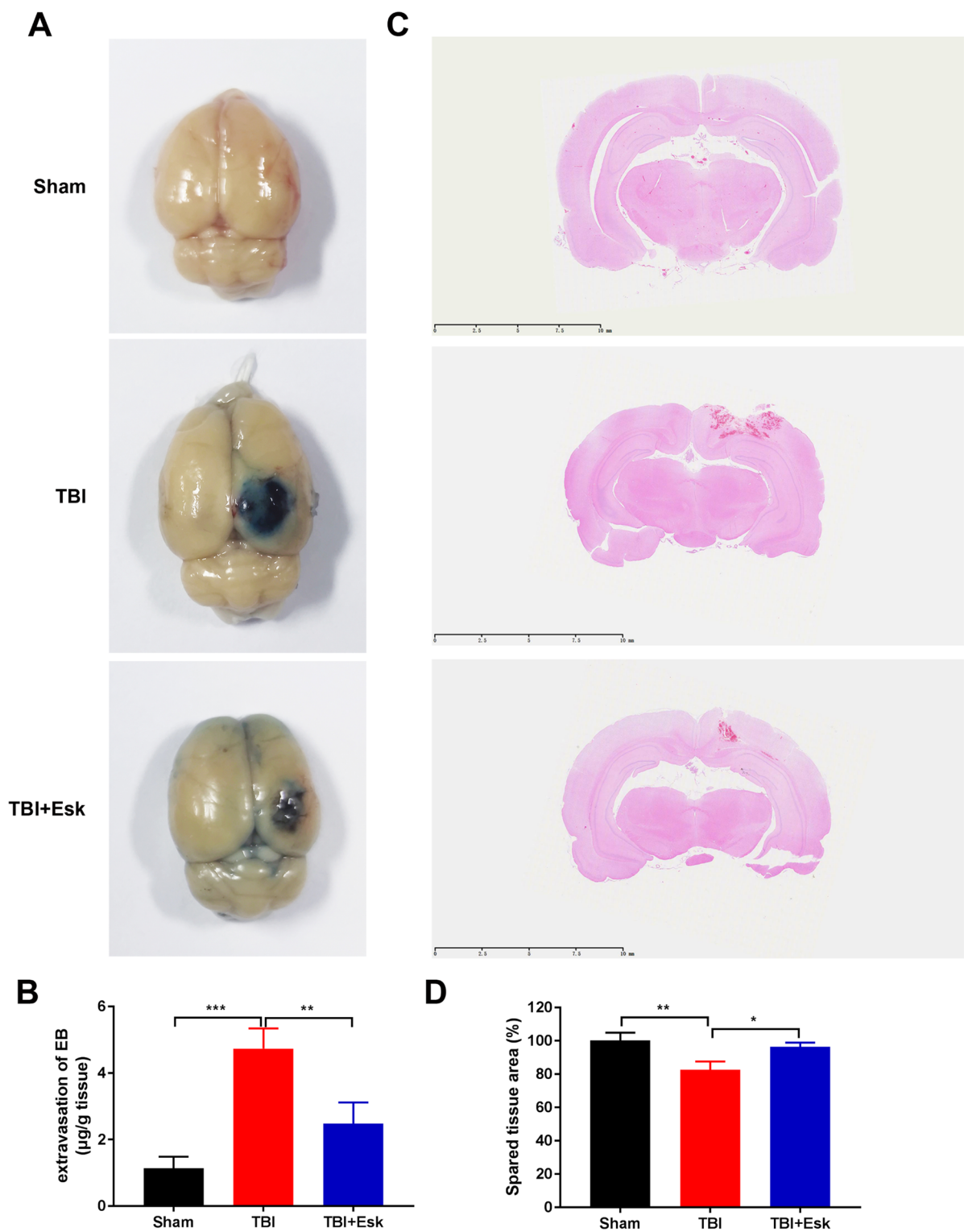


Fig. 1 Esketamine alleviates BBB disruption and brain tissue defects in TBI mice. **(A)** Representative images of EB extravasation in brain tissues from Sham, TBI, and TBI+Esk-treated mice, illustrating BBB permeability. **(B)** Quantification of EB's extravasation in brain tissues ($F = 33.11$). **(C)** Representative coronal brain sections stained with H&E, showing the extent of tissue defects. Scale bar = 10 mm. **(D)** Quantification of HE of spared brain tissues ($n = 3$, $F = 14.63$). Statistical significance: Data are represented as mean \pm SD of three independent experiments, ** p < 0.01 and *** p < 0.001

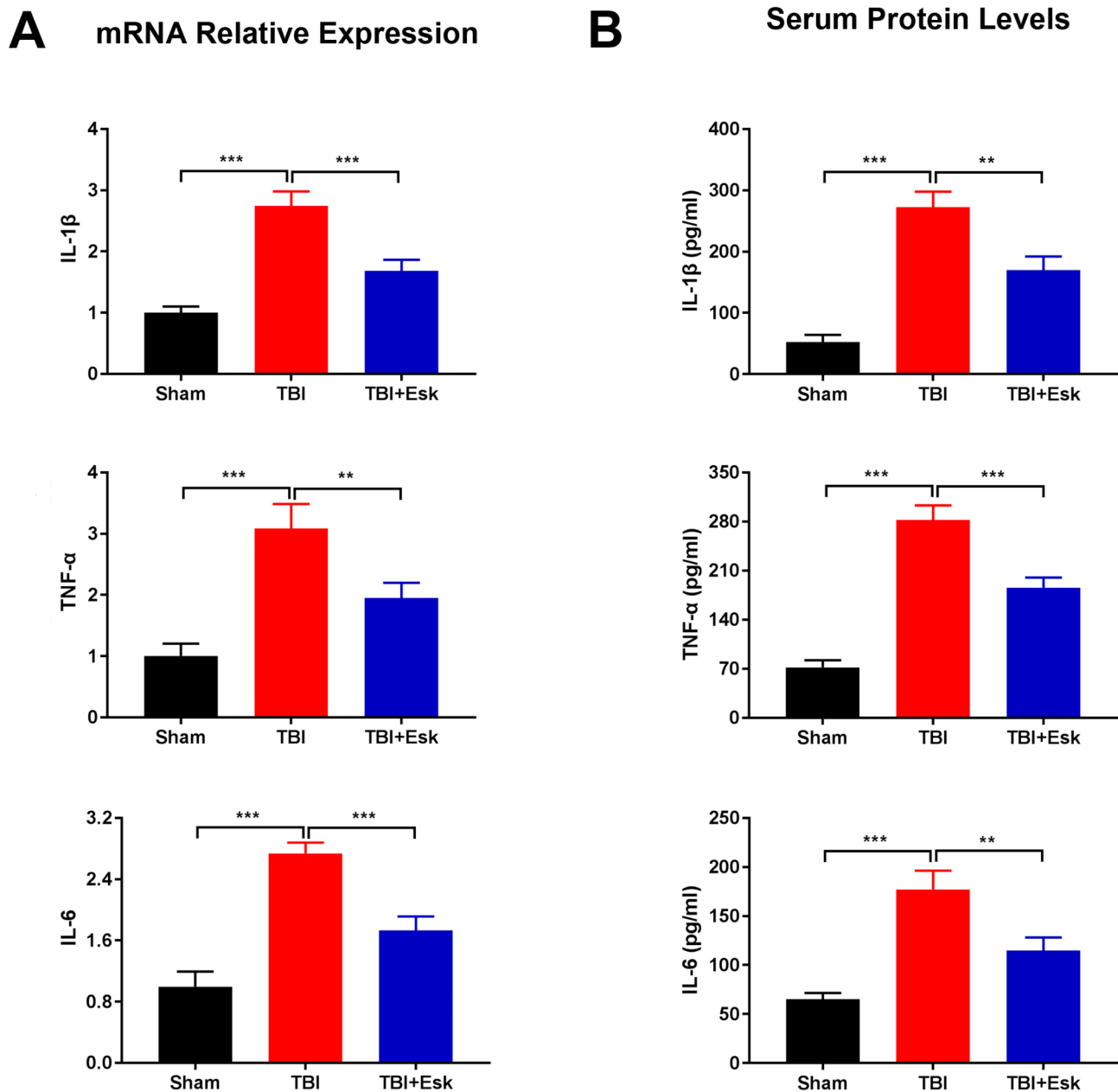


Fig. 2 Esketamine reduces inflammation markers in TBI mice. **(A)** Relative mRNA expression levels of inflammatory cytokines IL-1 β , TNF- α , and IL-6 in brain tissues ($F=70, 37.41, 74.83$, respectively). **(B)** Serum concentrations of IL-1 β , TNF- α , and IL-6 measured by ELISA ($F=84.34, 134, 48.25$, respectively). Statistical significance: Data are represented as mean \pm SD of three independent experiments, ** $p < 0.01$ and *** $p < 0.001$

Esketamine inhibits activation of CD4+T cells and regulates Th17/Treg cell balance in TBI mice

To investigate the immunomodulatory effects of esketamine in TBI, we utilized flow cytometry to assess the percentages of CD4+ T cells, Th17 cells, and Treg cells in both brain tissue and spleen of TBI mice. TBI resulted in a marked increase in the percentage of CD4+ T cells in both the brain and spleen compared to the sham group. Treatment with esketamine significantly reduced the proportion of CD4+ T cells in these tissues ($p < 0.01$ for

brain, $p < 0.01$ for spleen), suggesting a suppressive effect on T cell activation (Fig. 3A).

Further analysis focused on Th17 and Treg cell populations. TBI mice displayed an elevated percentage of Th17 cells in both brain and spleen tissue, indicating a heightened pro-inflammatory response. Esketamine treatment significantly decreased the proportion of Th17 cells in both tissues ($p < 0.001$ for brain, $p < 0.01$ for spleen), suggesting a reduction in inflammatory Th17 cell activation (Fig. 3B).

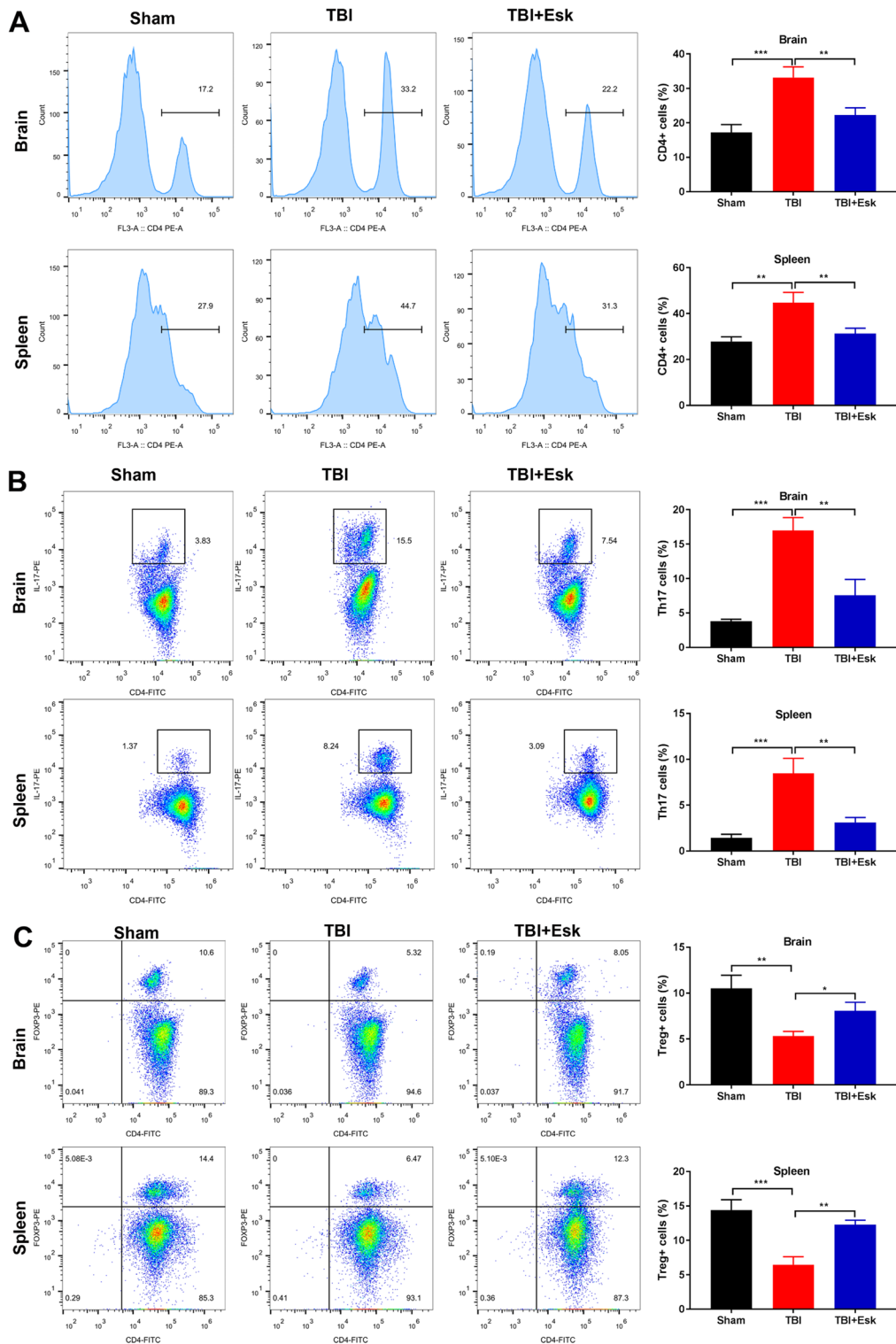


Fig. 3 Esketamine inhibits CD4+T cell activation and regulates Th17/Treg cell balance in TBI mice. Flow cytometry histograms showing (A) the percentage of CD4+T cells (F=31.76, 24.04), (B) Th17 (CD4+ IL-17+) cells (F=45.75, 38.07), and (C) Treg (CD4+ FOXP3+) cells in brain and spleen tissues from Sham, TBI, and TBI+ Esk-treated mice (F= 19.13, 37.55). Quantification of all cell percentages is shown on the right panel. Statistical significance: Data are represented as mean ± SD of three independent experiments, **p* < 0.05, ***p* < 0.01, and ****p* < 0.001

In contrast, TBI was associated with a decrease in Treg cell percentages in both brain and spleen (Fig. 3C). Treatment with esketamine effectively restored the Treg cell population, significantly increasing their proportion in TBI mice ($p < 0.01$ for brain, $p < 0.01$ for spleen), which suggests a shift towards an anti-inflammatory response.

Esketamine inhibits activation of CD4⁺T cells and regulates Th17 cell differentiation in vitro

In vitro experiments were performed to investigate the effects of esketamine on CD4⁺T cell activation and Th17/Treg cell differentiation. Esketamine treatment led to a dose-dependent reduction in the proportion of CD4⁺T cells after 24 h, with significant inhibition observed at higher concentrations ($p < 0.001$, Fig. 4A).

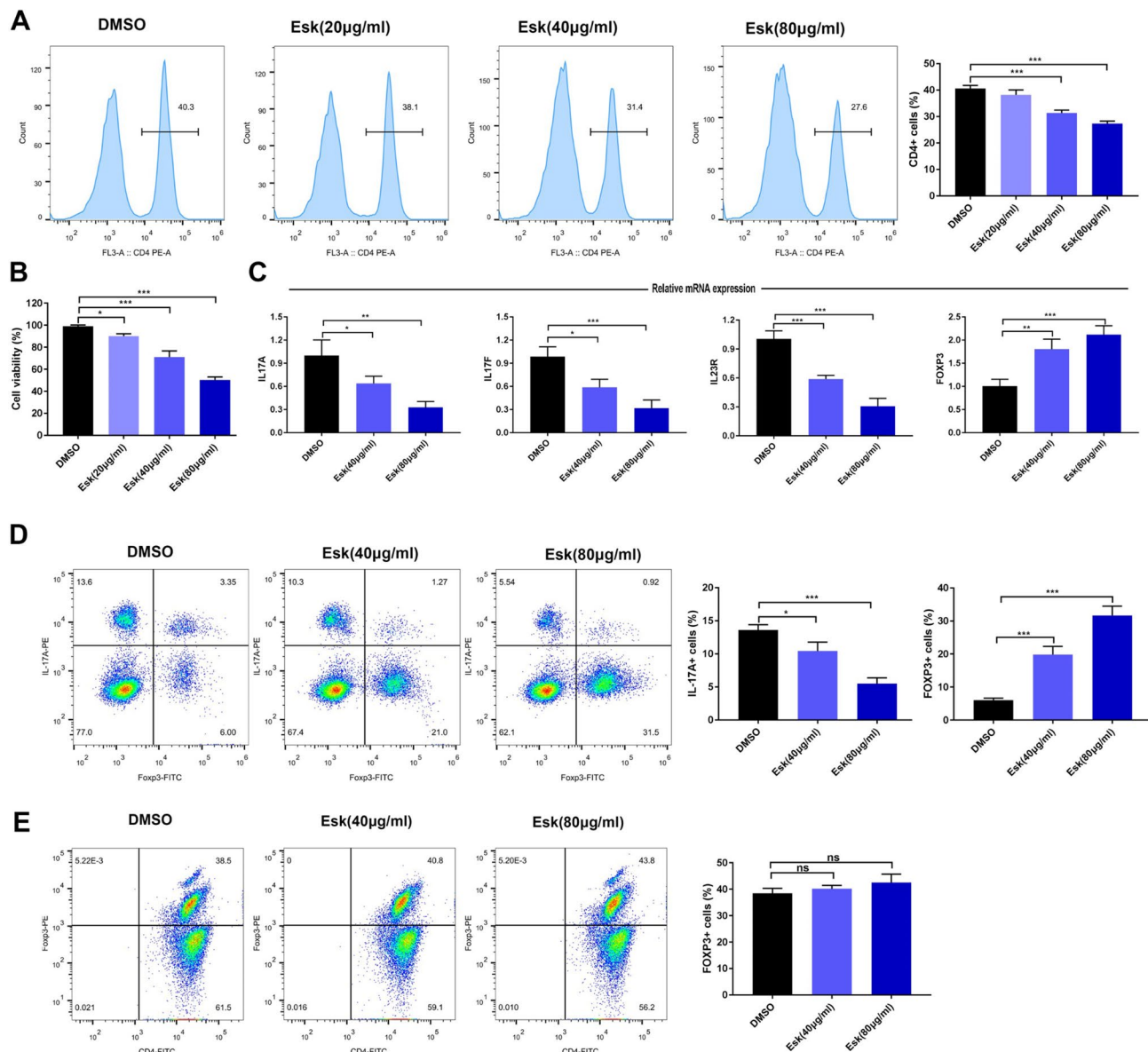


Fig. 4 Esketamine inhibits CD4⁺T cell activation and regulates Th17/Treg cell differentiation in vitro. **(A)** Flow cytometry histograms showing the percentage of CD4⁺T cells in splenocytes from TBI mice treated with different concentrations of esketamine (20, 40, and 80 µg/ml) for 24 h. Quantification of CD4⁺T cell percentages is shown on the right (F = 61.46). **(B)** Cell viability of CD4⁺T cells measured by CCK8 assay following esketamine treatment at varying concentrations (F = 126.8). **(C)** Relative mRNA expression levels of Th17-associated transcription factors (IL17A, IL17F, and IL23R) and Treg-associated transcription factor FOXP3 in CD4⁺T cells treated with esketamine (F = 18.77, 26.23, 72.43, 27.68, respectively). **(D)** Flow cytometry dot plots showing IL-17⁺Th17 cells and FOXP3⁺Treg cells under Th17-polarizing conditions with esketamine treatment at different doses. Quantification of IL-17⁺ and FOXP3⁺ cell percentages is shown on the right (F = 46.59, 102). **(E)** Flow cytometry histograms displaying FOXP3⁺Treg cells under Treg-polarizing conditions with esketamine treatment. Quantification of FOXP3⁺Treg cells is shown on the right (F = 2.419). Statistical significance: Data are represented as mean ± SD of three independent experiments, * $p < 0.05$, ** $p < 0.01$, *** $p < 0.001$, and ns for not significant

Cell viability, measured by the CCK8 assay, showed that esketamine significantly decreased CD4⁺T cell activity in a dose-dependent manner. Compared to the DMSO control group, esketamine at concentrations of 20, 40, and 80 µg/ml reduced cell viability with statistical significance ($p < 0.05$, $p < 0.01$, and $p < 0.001$, respectively; Fig. 4B).

To further investigate the effect of esketamine on Th17 cell differentiation, we measured mRNA expression levels of Th17-associated transcription factors (IL17A, IL17F, and IL23R) and the Treg-associated transcription factor FOXP3. Esketamine treatment at 20, 40, and 80 µg/ml significantly reduced the expression of IL17A (40 µg/ml: $p < 0.05$; 80 µg/ml: $p < 0.01$), IL17F (40 µg/ml: $p < 0.05$; 80 µg/ml: $p < 0.001$), and IL23R (40 µg/ml: $p < 0.001$; 80 µg/ml: $p < 0.001$) compared to the DMSO control, indicating a dose-dependent suppression of Th17 differentiation. In contrast, esketamine significantly increased FOXP3 expression in a dose-dependent manner (40 µg/ml: $p < 0.01$; 80 µg/ml: $p < 0.001$), suggesting enhanced Treg differentiation (Fig. 4C).

To assess whether esketamine directly regulates Th17 and Treg cell differentiation, naive CD4⁺T cells were cultured under Th17- or Treg-polarizing conditions. Under Th17-polarizing conditions, esketamine treatment significantly reduced the proportion of IL-17⁺ Th17 cells at 40 µg/ml ($p < 0.01$) and 80 µg/ml ($p < 0.001$) compared to the DMSO control. Concurrently, FOXP3⁺ Treg cells were significantly increased at 40 µg/ml and 80 µg/ml (both $p < 0.001$) (Fig. 4D).

Under Treg-polarizing conditions, however, esketamine did not significantly alter the proportion of FOXP3⁺ Treg cells at any tested dose (Fig. 4E). This suggests that esketamine specifically promotes Treg differentiation when cells are polarized towards a Th17 profile rather than in a general Treg-polarizing environment.

Neutralizing IL-17 A alleviates brain injury in TBI mice

To further investigate whether blocking IL-17 A could mitigate the progression of TBI, we administered esketamine alone or in combination with an anti-IL-17 A antibody to TBI mice. The therapeutic effectiveness of IL-17 A neutralization in conjunction with esketamine was assessed through molecular analyses and functional testing. Flow cytometry analysis revealed that esketamine treatment significantly reduced the percentage of Th17 cells in TBI mice compared to untreated TBI mice ($p < 0.001$; Fig. 5A). Furthermore, the combination of esketamine and anti-IL-17 A antibody (Esk+anti-IL-17 A) further decreased the proportion of Th17 cells compared to esketamine treatment alone, indicating enhanced inhibition of Th17 cell activation with IL-17 A neutralization ($p < 0.001$; Fig. 5A). Histological examination with H&E staining showed that brain

tissue abnormalities observed in TBI mice were reduced with esketamine treatment, and this effect was further enhanced in the Esk+anti-IL-17 A group, suggesting improved tissue integrity (Fig. 5B).

Functional assessments of neurological deficits, as indicated by the neurological severity score (NSS), demonstrated that TBI significantly increased NSS scores, reflecting substantial neurological impairment. Esketamine administration led to a notable improvement in neurological function (reduced NSS scores) in TBI mice, and the Esk+anti-IL-17 A group showed even greater improvement compared to the Esk-only group ($p < 0.05$ and $p < 0.001$; Fig. 5C).

Additionally, analysis of mRNA levels of inflammatory markers IL-1 β , TNF- α , and IL-6 demonstrated that TBI significantly upregulated these cytokines, indicating heightened inflammation. Esketamine treatment significantly reduced the mRNA expression of IL-1 β ($p < 0.001$), TNF- α ($p < 0.001$), and IL-6 ($p < 0.001$) compared to the TBI group. Furthermore, the combination treatment with Esketamine and anti-IL-17 A (Esk+anti-IL-17 A) led to even greater reductions in IL-1 β ($p < 0.05$ compared to Esk alone), TNF- α ($p < 0.01$ compared to Esk alone), and IL-6 ($p < 0.01$ compared to Esk alone), highlighting enhanced anti-inflammatory effects (Fig. 5D).

Esketamine inhibits Th17 differentiation via blocking STAT3 activation

Given that STAT3 activation is crucial for Th17 differentiation through cytokine signals (such as IL-6 and IL-23), we investigated the effect of esketamine on STAT3 activation in Th17 cells derived from CD4⁺T cells in the spleen of TBI mice. Western blot analysis revealed that esketamine significantly reduced the p-STAT3/STAT3 protein ratio in Th17 cells from TBI mice. Specifically, esketamine at 40 µg/ml ($p < 0.001$) and 80 µg/ml ($p < 0.001$), compared to the DMSO control, showed a dose-dependent inhibition of STAT3 activation (Fig. 6A). A similar effect was observed in Th17 cells differentiated from naive T cells in normal mice, with significant reductions in the p-STAT3/STAT3 ratio at both 40 µg/ml ($p < 0.001$) and 80 µg/ml ($p < 0.001$) compared to the DMSO control (Fig. 6B).

To further confirm the inactivation of STAT3 signaling, we examined STAT3 nuclear localization using immunofluorescence. Esketamine treatment significantly reduced nuclear accumulation of p-STAT3 in Th17 cells, with reductions observed at both 40 µg/ml ($p < 0.01$) and 80 µg/ml ($p < 0.001$) compared to the DMSO control (Fig. 6C).

To assess the functional impact of STAT3 inhibition on Th17 differentiation, we pretreated CD4⁺T cells with colivelin, a STAT3 activator, prior to esketamine administration. mRNA expression levels of Th17-related genes

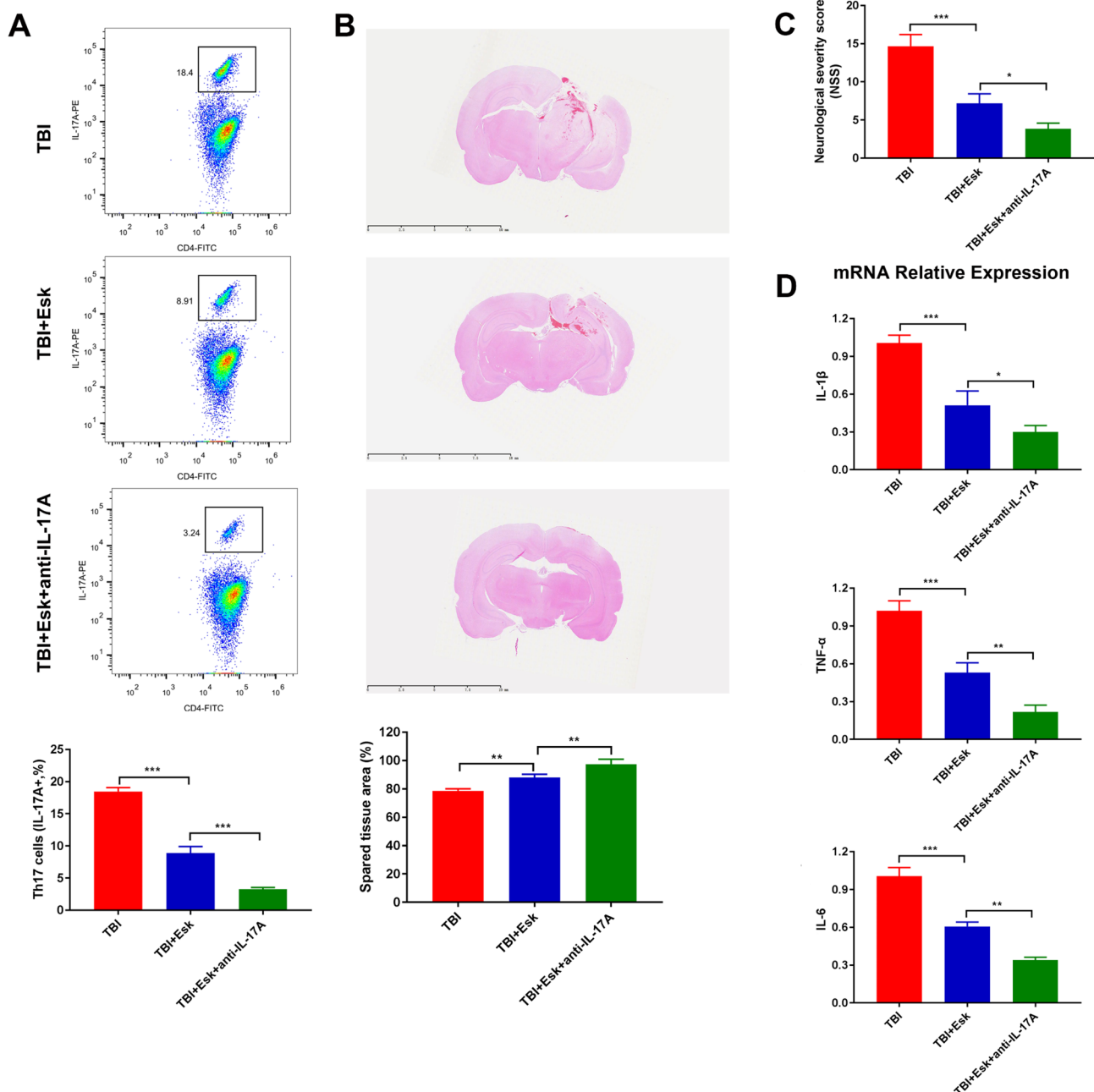


Fig. 5 Neutralizing IL-17 A enhances the therapeutic effects of Esketamine (Esk) in alleviating brain injury in TBI mice. **(A)** Flow cytometry histograms showing the percentage of Th17 (CD4+ IL-17 A+) cells in brain tissue from TBI, TBI + Esk, and TBI + Esk + anti-IL-17 A groups. Quantification of Th17 cell percentages is shown in lower panel ($F=356.9$). **(B)** Representative H&E-stained coronal brain sections from each group, showing the extent of tissue abnormalities ($F=40.73$). Scale bar = 10 mm. **(C)** Neurological severity scores (NSS) indicating neurological deficits in TBI, TBI + Esk, and TBI + Esk + anti-IL-17 A groups ($F=61.57$). **(D)** Relative mRNA expression levels of inflammatory cytokines IL-1 β , TNF- α , and IL-6 in brain tissue across groups ($F=60.96$, 95.29 , 156.1 , respectively). Statistical significance: Data are represented as mean \pm SD of three independent experiments, * $p < 0.05$, ** $p < 0.01$, *** $p < 0.001$

(IL17A, IL17E, and IL23R) were significantly reduced in esketamine-treated cells compared to the DMSO group (Fig. 6D). However, colivelin treatment partially reversed esketamine's inhibitory effect, with significant increases in IL17A ($p < 0.01$), IL17F ($p < 0.01$), and IL23R ($p < 0.05$) expression compared to the esketamine-alone group,

indicating that STAT3 activation is essential for maintaining Th17-related gene expression (Fig. 6D).

Esketamine promotes the transformation from M1 to M2 macrophage phenotype in TBI mice

Macrophages are crucial players in the immune response, involved in inflammation, defense, and the maintenance

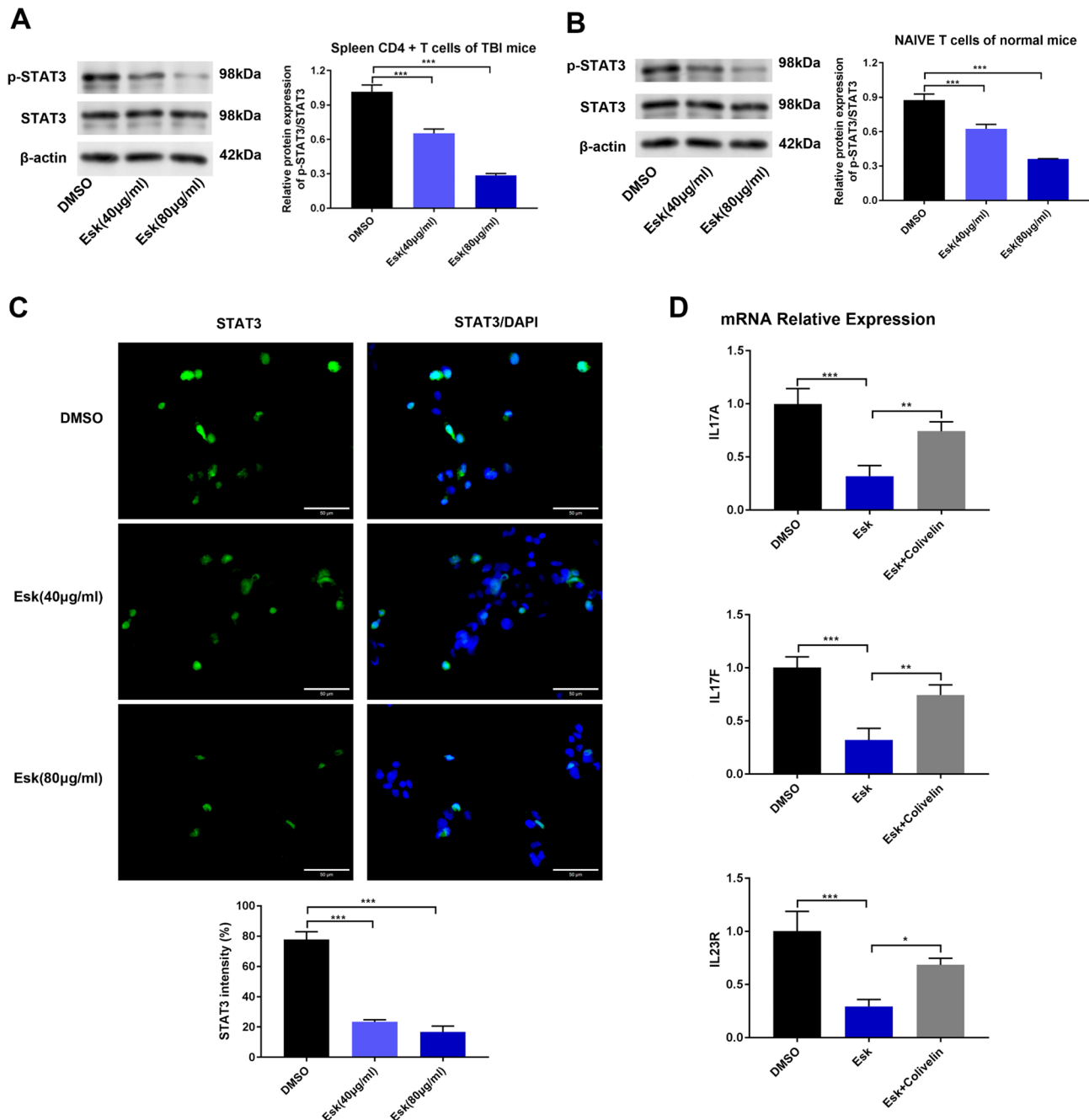


Fig. 6 Esketamine inhibits Th17 differentiation via suppression of STAT3 activation. **(A)** Western blot analysis of p-STAT3 and total STAT3 levels in CD4 + T cells from the spleen of TBI mice treated with DMSO or esketamine at 40 μ g/ml and 80 μ g/ml. Quantification of the p-STAT3/STAT3 ratio is shown on the right ($n=3$, $F=229.5$). **(B)** Western blot analysis of p-STAT3 and STAT3 in Th17 cells differentiated from naive T cells. Quantification of the p-STAT3/STAT3 ratio is shown on the right ($n=3$, $F=133.7$). **(C)** Immunofluorescence images showing STAT3 localization in Th17 cells treated with DMSO, 40 μ g/ml, or 80 μ g/ml esketamine. Quantification of nuclear STAT3 intensity is shown below. Scale bar = 50 μ m ($F=231.8$). **(D)** Relative mRNA expression levels of Th17-associated genes (IL17A, IL17F, and IL23R) in CD4 + T cells treated with DMSO, esketamine, or esketamine combined with colivelin (a STAT3 activator) ($F=27.22$, 33.93 , 26.91 respectively). Statistical significance: Data are represented as mean \pm SD of three independent experiments, * $p < 0.05$, ** $p < 0.01$, *** $p < 0.001$.

of tissue homeostasis. To investigate whether esketamine affects macrophage polarization in TBI mice, we assessed markers of the M1 and M2 macrophage phenotypes [20]. Immunofluorescence analysis showed that esketamine

treatment significantly reduced iNOS expression (M1 marker) while enhancing CD206 expression (M2 marker) ($p < 0.01$ and $p < 0.01$ for both markers, respectively; Fig. 7A). This suggests that esketamine promotes a shift

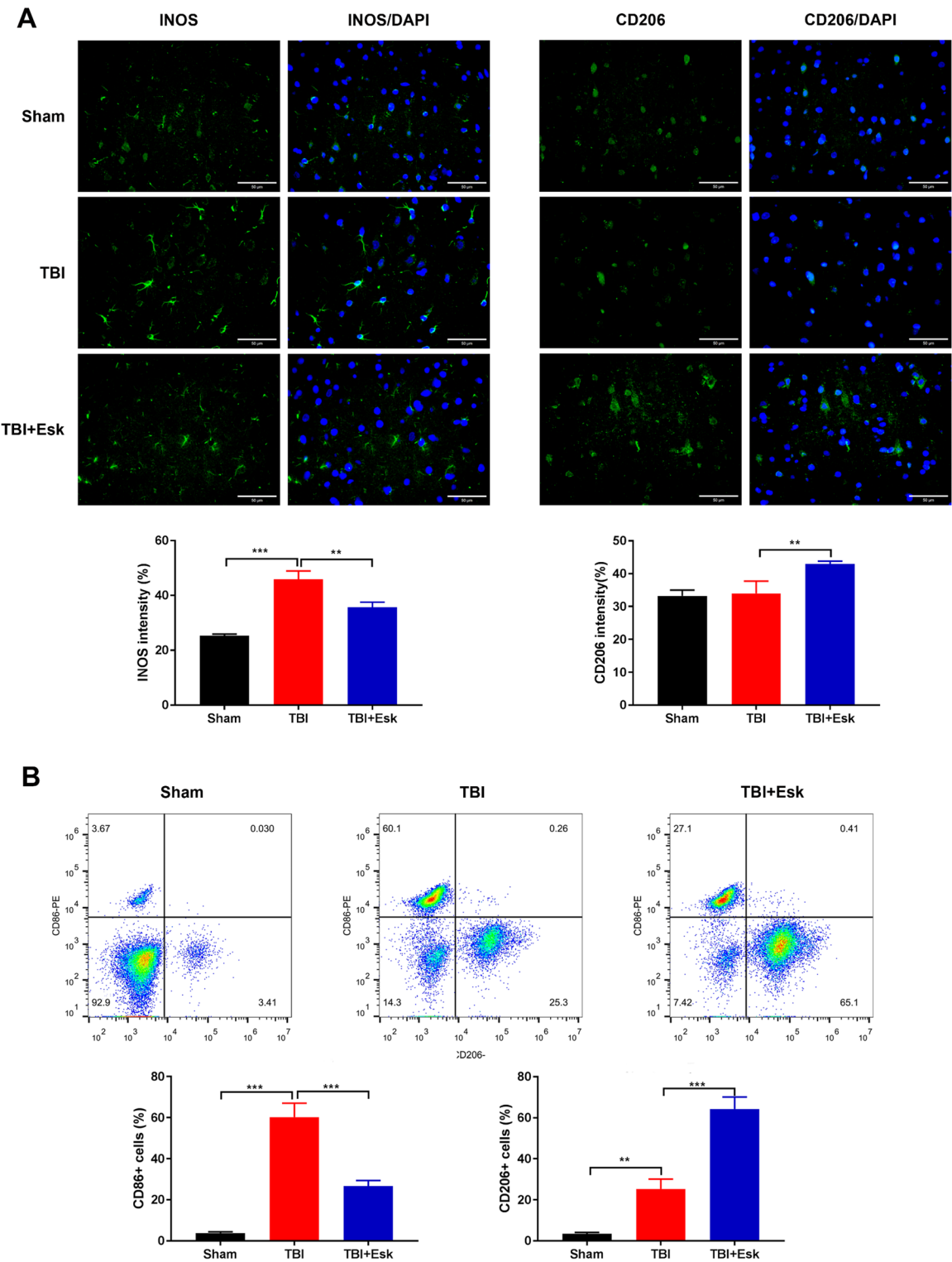


Fig. 7 Esketamine promotes M1 to M2 macrophage phenotype transformation in TBI mice. **(A)** Immunofluorescence images showing iNOS (M1 marker) and CD206 (M2 marker) expression in brain tissue from Sham, TBI, and TBI + Esk-treated mice. Quantification of iNOS and CD206 fluorescence intensity is shown below ($n=3$, $F=75.98$, 15.11). Scale bar = 50 μm . **(B)** Flow cytometry histograms showing the percentage of M1 (CD86+) and M2 (CD206+) macrophages in brain tissue from each group. Quantification of CD86+ and CD206+ cell percentages is shown below ($n=3$, $F=133.6$, 148.8). Statistical significance: Data are represented as mean \pm SD of three independent experiments, $**p < 0.01$ and $***p < 0.001$

towards the M2 anti-inflammatory phenotype in TBI-affected brain tissue.

Flow cytometry analysis further confirmed these results, showing a significant decrease in the percentage of M1 macrophages (CD86+) and a corresponding increase in the percentage of M2 macrophages (CD206+) following esketamine treatment ($p < 0.001$ for both CD86+ and CD206+; Fig. 7B). This shift from M1 to M2 macrophages after esketamine administration indicates a transformation towards an anti-inflammatory state, suggesting that esketamine may mitigate TBI progression by promoting macrophage polarization to the M2 phenotype.

Esketamine alleviates TBI progression via STAT3-mediated macrophage polarization in TBI mice

Phosphorylated STAT3 (p-STAT3) plays a role in regulating inflammation in neurons and microglia/macrophages, including inhibiting NLRP3 inflammasome-associated proteins [21]. Since we previously observed STAT3's involvement in Th17 cell differentiation in TBI, we next investigated whether STAT3 is also expressed in macrophages within TBI-affected brain tissue. Immunofluorescence analysis revealed STAT3 localization within infiltrating macrophages in the brain tissue of TBI mice (Fig. 8A).

Western blot analysis demonstrated that esketamine treatment significantly decreased the p-STAT3/STAT3 ratio in both RAW264.7 cells ($p < 0.001$) and bone marrow-derived macrophages (BMDMs; $p < 0.001$) compared to the DMSO control (Fig. 8B and C), indicating reduced STAT3 activation in macrophages following esketamine stimulation.

To examine the role of STAT3 in macrophage polarization, we pretreated TBI mice with colivelin, a STAT3-specific agonist, before esketamine administration. Analysis of M1 (iNOS) and M2 (Arg1, CD206) markers by qRT-PCR showed that esketamine significantly reduced iNOS expression ($p < 0.001$), while increasing Arg1 ($p < 0.001$) and CD206 ($p < 0.01$) expression, indicative of M2 polarization. Colivelin pretreatment reversed these effects, increasing iNOS ($p < 0.01$), and reducing Arg1 ($p < 0.05$) and CD206 ($p < 0.01$) expression levels compared to the esketamine group alone (Fig. 8D).

Functional outcomes were assessed through NSS. Esketamine treatment significantly lowered NSS scores, indicating improved neurological function ($p < 0.001$). However, colivelin administration attenuated this improvement, resulting in higher NSS scores compared to esketamine treatment alone ($p < 0.05$; Fig. 8E).

Lastly, we evaluated the effect of STAT3 modulation on inflammation by measuring mRNA expression levels of pro-inflammatory cytokines IL-1 β , TNF- α , and IL-6. Esketamine treatment significantly reduced these

inflammatory markers (all $p < 0.001$), while colivelin pretreatment partially reversed this reduction, leading to moderately higher levels of IL-1 β (all $p < 0.001$), TNF- α ($p < 0.05$), and IL-6 ($p < 0.01$) compared to the esketamine group (Fig. 8F).

Esketamine inhibits Th17 differentiation and M1 polarization via STAT3-mediated Glycolysis

To explore whether esketamine affects STAT3-mediated glycolysis, we analyzed the expression of key glycolytic genes in Th17 cells and RAW264.7 macrophages. RT-qPCR results showed that esketamine treatment significantly reduced the expression of glycolytic genes, including Hk2, Pgk1, Aldoa, Pkm2, and Ldha, compared to the DMSO control, in both Th17 cells and RAW264.7 cells ($p < 0.001$ for most comparisons; Fig. 9A). Specifically, esketamine reduced the expression of these genes. However, colivelin, a STAT3 activator, partially restored the expression of these glycolytic genes in the Esk + colivelin group, demonstrating that esketamine inhibits STAT3-mediated glycolytic metabolism (Fig. 9A).

Given the esketamine link between glycolysis and macrophage activity, we further examined whether esketamine influences Th17 differentiation and M1 macrophage polarization through glycolysis modulation. To test this, we used 2-deoxyglucose (2-DG), a glycolytic inhibitor, in combination with esketamine and colivelin. Flow cytometry analysis revealed that colivelin treatment increased the percentage of M1 (CD86+) macrophages and Th17 (IL-17 A+) cells by approximately 3-fold compared to esketamine alone ($p < 0.001$) and decreased the percentage of M2 (CD206+) macrophages ($p < 0.01$). However, the addition of 2-DG to the Esk + colivelin treatment partially reversed these effects, leading to a decrease in M1 (CD86+) and Th17 (IL-17 A+) cells ($p < 0.05$) and an increase in M2 (CD206+) macrophages ($p < 0.01$, Fig. 9B).

Discussion

Our study reveals that esketamine exerts potent neuroprotective effects in a TBI model by modulating key inflammatory pathways, specifically targeting Th17 differentiation, M1 macrophage polarization, and STAT3-mediated glycolysis. This investigation underscores the therapeutic potential of esketamine, an NMDA receptor antagonist, in ameliorating TBI-associated neuroinflammation through its multifaceted impacts on immune cell dynamics and metabolic processes.

One of the most prominent findings in our study is the significant reduction of pro-inflammatory cytokines (IL-1 β , TNF- α , and IL-6) in both brain tissue and serum of TBI mice treated with esketamine. This aligns with previous research indicating esketamine's influence on immune cells like T cells and macrophages. In

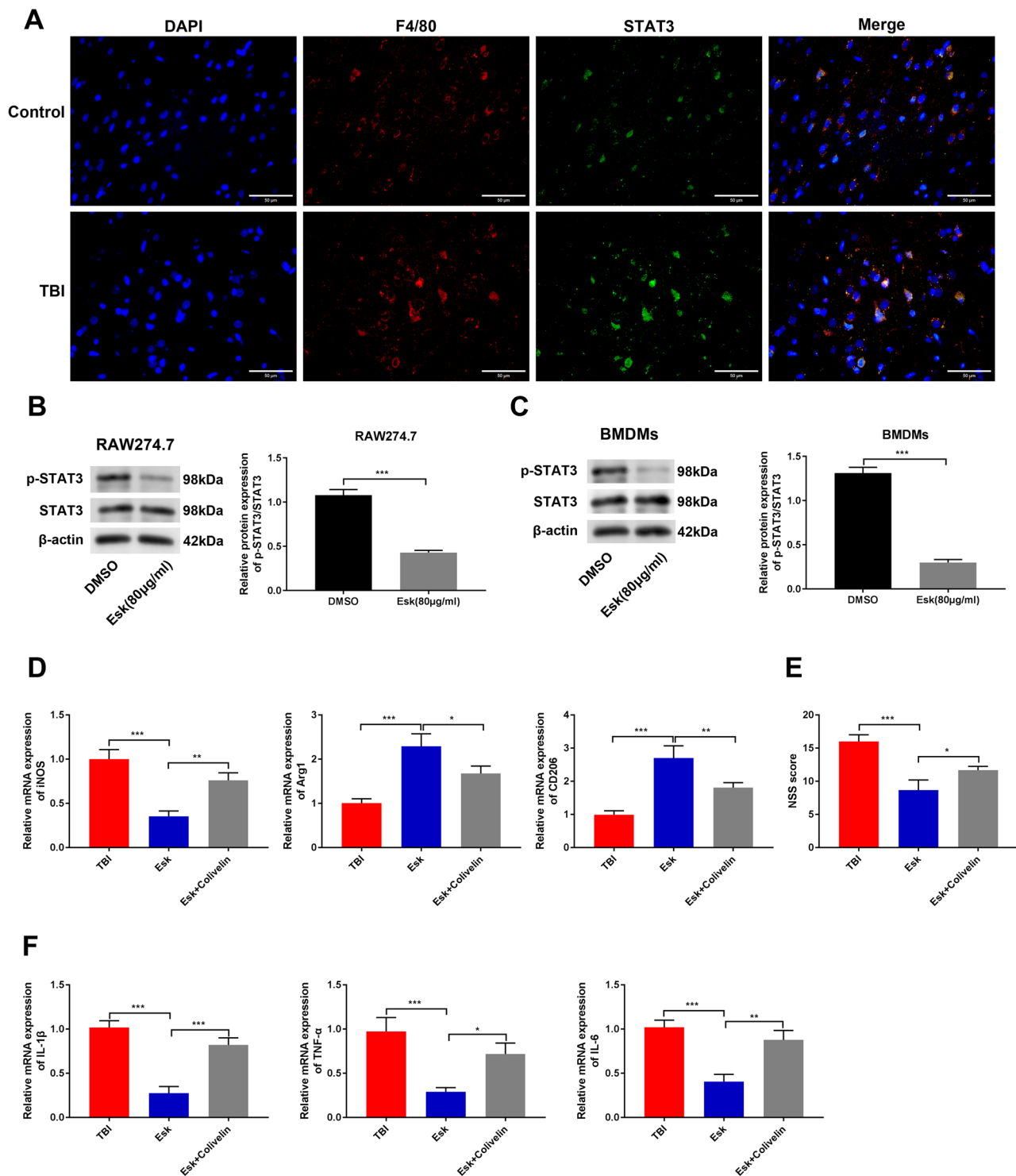


Fig. 8 Esketamine alleviates TBI progression via STAT3-mediated macrophage polarization. **(A)** Immunofluorescence images showing STAT3 localization in F4/80+ macrophages in the brain tissue of Control and TBI mice ($n=3$). Scale bar = 50 μm . **(B, C)** Western blot analysis of p-STAT3 and STAT3 in RAW264.7 cells **(B)** and bone BMDMs **(C)** treated with DMSO or 80 $\mu\text{g/ml}$ Esk. Quantification of the p-STAT3/STAT3 ratio is shown on the right ($n=3$). **(D)** Relative mRNA expression levels of M1 marker (iNOS) and M2 markers (Arg1, CD206) in brain tissue of TBI mice treated with Esk or Esk + colivelin (a STAT3 agonist) ($F=43.07, 31.49, 37.9$, respectively). **(E)** Nss score in TBI mice treated with Esk or Esk + colivelin ($F=33.36$). **(F)** Relative mRNA expression levels of inflammatory cytokines (IL-1 β , TNF- α , and IL-6) in TBI mice treated with Esk or Esk + colivelin ($F=74.12, 25.44, 37.41$, respectively). Statistical significance: Data are represented as mean \pm SD of three independent experiments, * $p < 0.05$, ** $p < 0.01$, *** $p < 0.001$

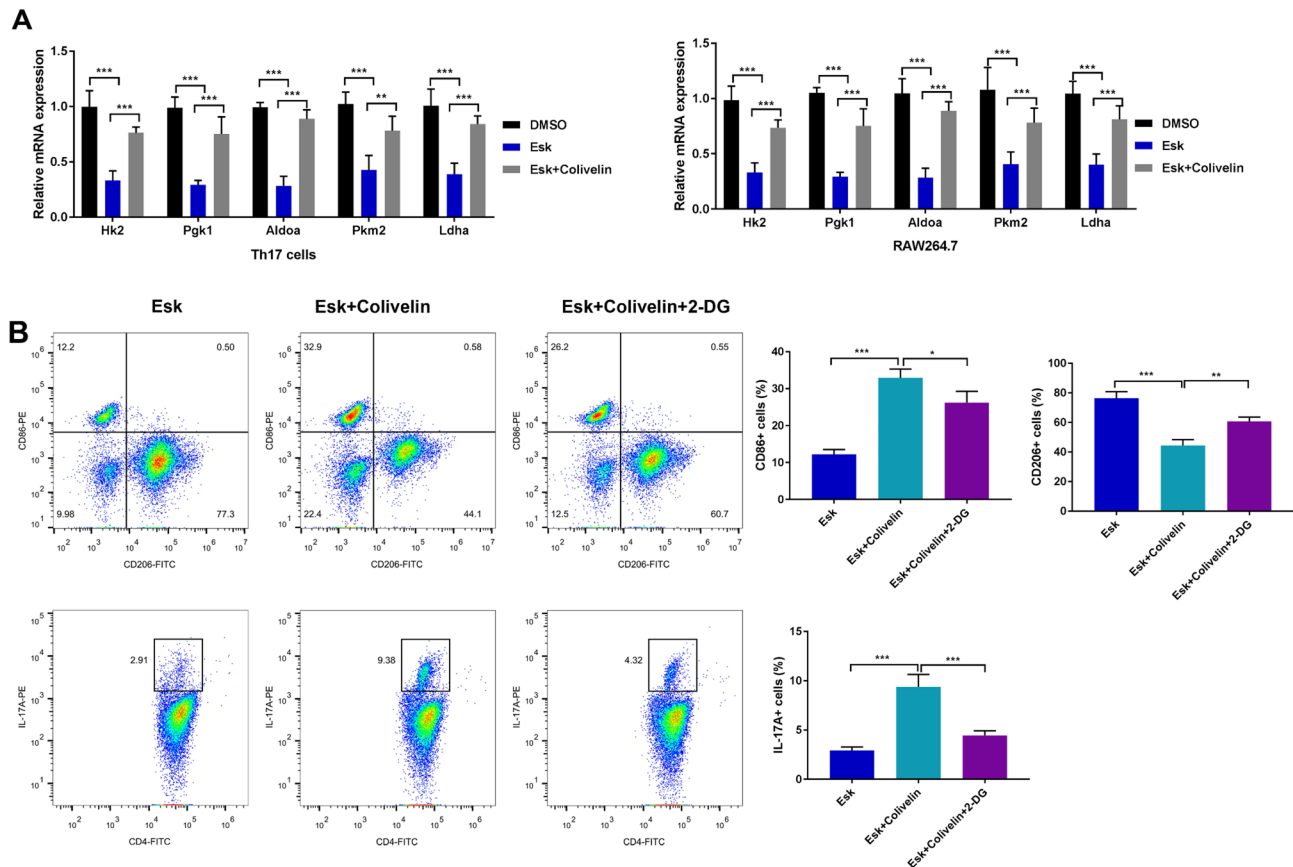


Fig. 9 Esketamine inhibits Th17 differentiation and M1 polarization via STAT3-mediated glycolysis. **(A)** Relative mRNA expression levels of glycolytic genes (Hk2, Pgk1, Aldoa, Pkm2, and Ldha) in Th17 cells and RAW264.7 macrophages treated with DMSO, Esk, or Esk + colivelin. Expression levels were normalized to the DMSO group. Statistical significance: * $p < 0.05$, ** $p < 0.01$, *** $p < 0.001$. **(B)** Flow cytometry dot plots showing the percentages of M1 (CD86+) and M2 (CD206+) macrophages and IL-17 A+ Th17 cells in cells treated with Esk, Esk + colivelin, or Esk + colivelin + 2-DG (a glycolysis inhibitor). Quantification of CD86+, CD206+, and IL-17 A+ cell percentages is shown on the right ($F = 58.86, 51.81, 52.91$). Statistical significance: Data are represented as mean \pm SD of three independent experiments, * $p < 0.05$, ** $p < 0.01$, *** $p < 0.001$

models of stress-induced depression, esketamine normalized anti-inflammatory cytokines (IL-4, IL-10, IL-24, IL-37), promoting an anti-inflammatory response [22]. It also suppresses microglial activation, reducing neuroinflammation and supporting neuroprotection [23]. In patients with treatment-resistant depression, esketamine decreased pro-inflammatory cytokines (IL-6, TNF- α) and increased anti-inflammatory cytokines (IL-4). This dual modulation contributes to its overall anti-inflammatory effect. Importantly, our study demonstrates that esketamine suppresses the pro-inflammatory Th17 cell response while promoting regulatory T cell (Treg) expansion. This shift in T cell balance may be crucial for reducing neuroinflammation, as Th17 cells have been implicated in the exacerbation of TBI-related neurodegeneration, whereas Tregs contribute to anti-inflammatory and tissue-repairing effects [24]. The observed reduction in IL-1 β , TNF- α , and IL-6 levels further supports esketamine's potential to attenuate inflammation-induced secondary injury in TBI [25, 26].

Our data indicate that esketamine exerts its anti-inflammatory effects partly through inhibition of the STAT3 pathway. STAT3 is crucial for Th17 cell differentiation and activation, driven by cytokines like IL-6 and IL-23, which induce STAT3 to promote Th17-specific genes (IL-17 A, IL-17 F). This process relies on enhanced glycolysis for energy and biosynthesis. Similarly, STAT3 activation in macrophages supports M1 polarization, also glycolysis dependent. Thus, STAT3 integrates key signaling and metabolic pathways vital for Th17 and M1 macrophage functions [27, 28]. The inhibition of STAT3 phosphorylation by esketamine in Th17 cells correlates with reduced expression of Th17-associated genes (IL17A, IL17F, and IL23R), suggesting that esketamine effectively disrupts the metabolic requirements for Th17 differentiation. Additionally, our in vitro experiments show that blocking STAT3 activity reduces glycolytic gene expression in both Th17 cells and RAW264.7 macrophages, reinforcing the link between STAT3 signaling, glycolysis, and Th17/M1 polarization [29, 30]. This

mechanism is further supported by our use of the glycolysis inhibitor 2-DG, which enhances esketamine's ability to reduce M1 macrophage and Th17 cell proportions, suggesting that targeting glycolysis can augment the therapeutic effects of esketamine.

Another key finding of this study is the shift from M1 to M2 macrophage phenotypes following esketamine treatment. TBI often leads to an accumulation of M1 macrophages, which exacerbate inflammation and tissue damage, whereas M2 macrophages are associated with anti-inflammatory and reparative roles [31]. Our results demonstrate that esketamine promotes M2 polarization, as indicated by increased expression of the M2 marker CD206 and decreased expression of the M1 marker iNOS. These effects are mediated through STAT3 signaling, as shown by the reversal of esketamine's polarization effects upon administration of colivelin, a STAT3 agonist. This finding aligns with previous studies suggesting that STAT3 activation supports M1 polarization, while its inhibition may favor M2 macrophage differentiation [29, 32, 33]. Consequently, esketamine's ability to modulate macrophage polarization highlights a potential pathway to mitigate chronic inflammation in TBI, fostering an environment conducive to tissue repair and functional recovery.

While these findings shed light on esketamine's multifaceted roles in TBI, several limitations warrant consideration. First, our study is limited to an animal model, and differences in human immune responses could influence the translatability of these results. Furthermore, STAT3 signaling plays broad roles in various immune pathways, including NF- κ B activation, which also contributes to TBI-related inflammation [34]. Thus, while esketamine's inhibition of STAT3 reduces neuroinflammation, additional work is needed to isolate its effects on other immune pathways. Finally, our model does not address long-term outcomes of TBI and esketamine's effects on cognitive function and neurodegeneration, which are important aspects for future studies.

Conclusions

Our findings indicate that esketamine provides neuroprotection, with effects that go beyond NMDA receptor modulation, through a STAT3-mediated pathway affecting both glycolysis and immune cell polarization. By inhibiting STAT3 phosphorylation, esketamine reduces glycolytic activity, which in turn suppresses the differentiation of Th17 cells and M1 macrophages. At the same time, it promotes Tregs and M2 macrophages, supporting an environment conducive to anti-inflammatory and tissue-repair processes. This dual action on T cell and macrophage subsets demonstrates esketamine's broad influence on adaptive and innate immune responses,

helping to reduce neuroinflammation and preserve tissue integrity in TBI.

Supplementary Information

The online version contains supplementary material available at <https://doi.org/10.1186/s12868-025-00941-z>.

Supplementary Material 1

Supplementary Material 2

Acknowledgements

Not applicable.

Author contributions

Technical and conceptual ideas in this work were conceived by YL, ZG and XL. LZ and XY collected experiments' data. JZ, XZ and XL performed data analysis and data interpretation. YL and ZG wrote the manuscript. All authors contributed to the article and approved the submitted version.

Funding

The study was supported by scientific research program of Wuxi health commission (M202233) and Top talent support program for young and middle-aged people of Wuxi health committee (BJ2023110).

Data availability

All data generated or analyzed during this study are included in this published article and its supplementary information files.

Declarations

Ethics approval and consent to participate

All the operations followed the National Institutes of Health Guidelines for the Care and Use of Laboratory Animals and ARRIVE Guidelines pertaining to animal experimentation. All animal experiments were approved by the Animal Ethics Committee of 904th Hospital of The Joint Logistics Support Force of the PLA (20241201).

Consent for publication

Not applicable.

Competing interests

The authors declare no competing interests.

Received: 4 December 2024 / Accepted: 25 February 2025

Published online: 07 March 2025

References

1. Ma D, Wang N, Fan X, Zhang L, Luo Y, Huang R et al. Protective effects of Cornel iridoid glycoside in rats after traumatic brain injury. 2018;43(4):959–71.
2. Haarbauer-Krupa J, Pugh MJ, Prager EM, Harmon N, Wolfe J, Yaffe K. Epidemiology of chronic effects of traumatic brain injury. *J Neurotrauma*. 2021;38(23):3235–47.
3. Riggio S. Traumatic brain injury and its neurobehavioral sequelae. *Neurol Clin*. 2011;29(1):35–47. vii.
4. Chen J, Li M, Chen L, Chen W, Zhang C, Feng Y, et al. The effect of controlled decompression for severe traumatic brain injury: A randomized, controlled trial. *Front Neurol*. 2020;11:107.
5. Hutchinson PJ, Kolias AG, Timofeev IS, Corteen EA, Czosnyka M, Timothy J, et al. Trial of decompressive craniectomy for traumatic intracranial hypertension. *N Engl J Med*. 2016;375(12):1119–30.
6. Cooper DJ, Nichol AD, Bailey M, Bernard S, Cameron PA, Pili-Floury S, et al. Effect of early sustained prophylactic hypothermia on neurologic outcomes among patients with severe traumatic brain injury: the POLAR randomized clinical trial. *JAMA*. 2018;320(21):2211–20.

7. Bao W, Lin Y, Chen Z. The peripheral immune system and traumatic brain injury: insight into the role of T-helper cells. *Int J Med Sci*. 2021;18(16):3644–51.
8. Celorrio M, Shumilov K, Friess SH. Gut microbial regulation of innate and adaptive immunity after traumatic brain injury. *Neural Regeneration Res*. 2024;19(2):272–6.
9. Yu F, Wang Y, Stetler AR, Leak RK, Hu X. Phagocytic microglia and macrophages in brain injury and repair. 2022;28(9):1279–93.
10. Xiong XY, Liu L, Yang QW. Functions and mechanisms of microglia/macrophages in neuroinflammation and neurogenesis after stroke. *Prog Neurobiol*. 2016;142:23–44.
11. Casoni D, Spadavecchia C, Wampfler B, Thormann W, Levisonnois OL. Clinical and Pharmacokinetic evaluation of S-ketamine for intravenous general anaesthesia in horses undergoing field castration. *Acta Vet Scand*. 2015;57(1):21.
12. Turner EH. Esketamine for treatment-resistant depression: seven concerns about efficacy and FDA approval. *Lancet Psychiatry*. 2019;6(12):977–9.
13. Li Y, Wu ZY, Zheng WC, Wang JX, Yue X, Song RX, et al. Esketamine alleviates postoperative cognitive decline via stimulator of interferon genes/TANK-binding kinase 1 signaling pathway in aged rats. *Brain Res Bull*. 2022;187:169–80.
14. Li H, Hu W, Wu Z, Tian B, Ren Y, Zou X. Esketamine improves cognitive function in sepsis-associated encephalopathy by inhibiting microglia-mediated neuroinflammation. *Eur J Pharmacol*. 2024;983:177014.
15. Du H, Li CH, Gao RB, Cen XQ, Li P. Ablation of GSDMD attenuates neurological deficits and neuropathological alterations after traumatic brain injury. *Front Cell Neurosci*. 2022;16:915969.
16. Tang Y, Liu Y, Zhou H, Lu H, Zhang Y, Hua J, et al. Esketamine is neuroprotective against traumatic brain injury through its modulation of autophagy and oxidative stress via AMPK/mTOR-dependent TFEB nuclear translocation. *Exp Neurol*. 2023;366:114436.
17. Pineda-Torra I, Gage M, de Juan A, Pello OM. Isolation, Culture, and Polarization of Murine Bone Marrow-Derived and Peritoneal Macrophages. *Methods in molecular biology* (Clifton, NJ). 2015;1339:101–9.
18. Yao M, Gao F, Xu R, Zhang J, Chen Y, Guan F. A dual-enzymatically cross-linked injectable gelatin hydrogel loaded with BMSC improves neurological function recovery of traumatic brain injury in rats. *Biomaterials Sci*. 2019;7(10):4088–98.
19. Shen J, Xin W, Li Q, Gao Y, Yuan L, Zhang J. Methylene blue reduces neuronal apoptosis and improves Blood-Brain barrier integrity after traumatic brain injury. *Front Neurol*. 2019;10:1133.
20. Ransohoff RM. A polarizing question: do M1 and M2 microglia exist? *Nat Neurosci*. 2016;19(8):987–91.
21. Zhu H, Jian Z, Zhong Y, Ye Y, Zhang Y, Hu X, et al. Janus kinase Inhibition ameliorates ischemic stroke injury and neuroinflammation through reducing NLRP3 inflammasome activation via JAK2/STAT3 pathway Inhibition. *Front Immunol*. 2021;12:714943.
22. Chen H, Zhao X, Ma X, Ma H, Zhou C, Zhang Y et al. Effects of Esketamine and Fluoxetine on depression-like behaviors in chronic variable stress: a role of plasma inflammatory factors. *Front Psychiatry*. 2024;15.
23. Wen Y, Xu J, Shen J, Tang Z, Li S, Zhang Q, et al. Esketamine prevents post-operative emotional and cognitive dysfunction by suppressing microglial M1 polarization and regulating the BDNF-TrkB pathway in ageing rats with preoperative sleep disturbance. *Mol Neurobiol*. 2024;61(8):5680–98.
24. Machhi J, Kevadiya BD, Muhammad IK, Herskovitz J, Olson KE, Mosley RL, et al. Harnessing regulatory T cell neuroprotective activities for treatment of neurodegenerative disorders. *Mol Neurodegeneration*. 2020;15(1):32.
25. Grgac I, Herzer G, Voelckel WG, Secades JJ, Trimmel H. Neuroprotective and neuroregenerative drugs after severe traumatic brain injury. *Wien Klin Wochenschr*. 2024;136(23–24):662–73.
26. Ooi SZY, Spencer RJ, Hodgson M, Mehta S, Phillips NL, Preest G, et al. Interleukin-6 as a prognostic biomarker of clinical outcomes after traumatic brain injury: a systematic review. *Neurosurg Rev*. 2022;45(5):3035–54.
27. Damasceno LEA, Prado DS, Veras FP, Fonseca MM, Toller-Kawahisa JE, Rosa MH, et al. PKM2 promotes Th17 cell differentiation and autoimmune inflammation by fine-tuning STAT3 activation. *J Exp Med*. 2020;217(10):e20190613.
28. Liu C, Zhou X. TREM2 impairs Glycolysis to interrupt microglial M1 polarization and inflammation via JAK2/STAT3 Axis. *Cell Biochem Biophys*. 2024. <https://doi.org/10.1007/s12013-024-01520-5>. Epub ahead of print.
29. Xia T, Zhang M, Lei W, Yang R, Fu S, Fan Z et al. Advances in the role of STAT3 in macrophage polarization. *Front Immunol*. 2023;14.
30. Kitabayashi C, Fukada T, Kanamoto M, Ohashi W, Hojyo S, Atsumi T, et al. Zinc suppresses Th17 development via Inhibition of STAT3 activation. *Int Immunol*. 2010;22(5):375–86.
31. Enam SF, Kader SR, Bodkin N, Lyon JG, Calhoun M, Azrak C, et al. Evaluation of M2-like macrophage enrichment after diffuse traumatic brain injury through transient interleukin-4 expression from engineered mesenchymal stromal cells. *J Neuroinflamm*. 2020;17(1):197.
32. Lei J, Shu Z, Zhu H, Zhao L. AMPK regulates M1 macrophage polarization through the JAK2/STAT3 signaling pathway to attenuate airway inflammation in Obesity-Related asthma. *Inflammation*. 2024;48(1):372–92.
33. Rébé C, Ghiringhelli F. STAT3, a master regulator of Anti-Tumor immune response. *Cancers [Internet]*. 2019; 11(9).
34. Babkina II, Sergeeva SP, Gorbacheva LR. The role of NF-κB in neuroinflammation. *Neurochemical J*. 2021;15(2):114–28.

Publisher's note

Springer Nature remains neutral with regard to jurisdictional claims in published maps and institutional affiliations.